

Supplementary Information

(Y,Tb,Eu)₂O₃ monospheres for highly fluorescent films and transparent hybrid films of color tunable emission

Qi Zhu¹, Mei Xiong¹, Ji-Guang Li^{1,2*}, Weigang Liu¹, Zhihao Wang¹, Xiaodong Li¹, and Xudong Sun¹

¹*Key Laboratory for Anisotropy and Texture of Materials (Ministry of Education), School of Materials and Metallurgy, Northeastern University, Shenyang, Liaoning 110819, China*

²*Advanced Materials Processing Unit, National Institute for Materials Science, Tsukuba, Ibaraki 305-0044, Japan*

*E-mail: LI.Jiguang@nims.go.jp

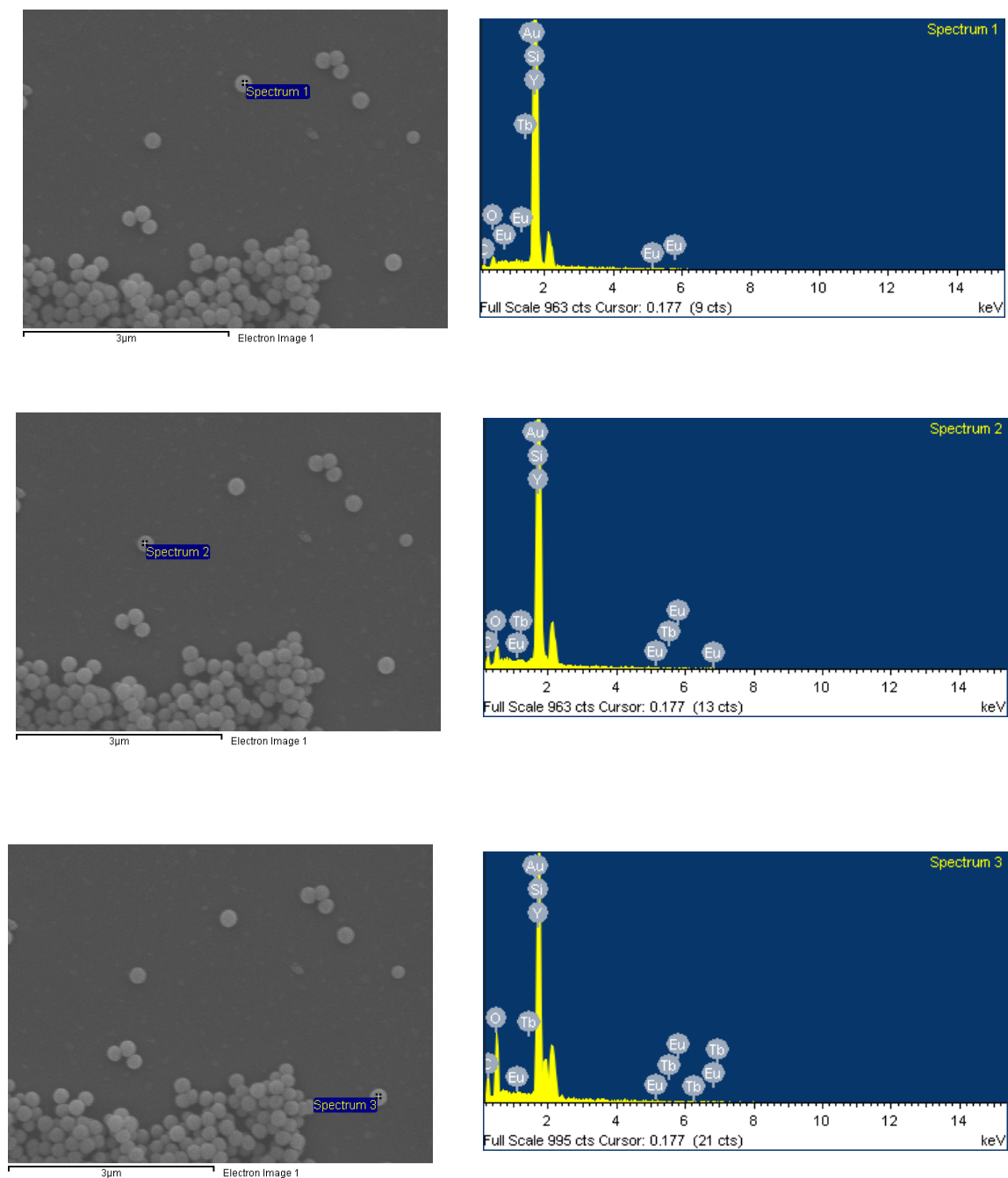


Fig. S1 Typical EDX spectra randomly taken from three single spheres of $(Y_{0.95}Tb_{0.02}Eu_{0.03})(OH)CO_3 \cdot nH_2O$ sample, where the Y, Tb, Eu, C, and O signals are clearly observed along with those for Au and Si. The latter two elements are originated from the gold sputtered on the sample surface to increase conductivity and the Si substrate, respectively. The above results indicate that the precursor particles synthesized by the urea-based homogeneous precipitation (UBHP) method are solid solutions.

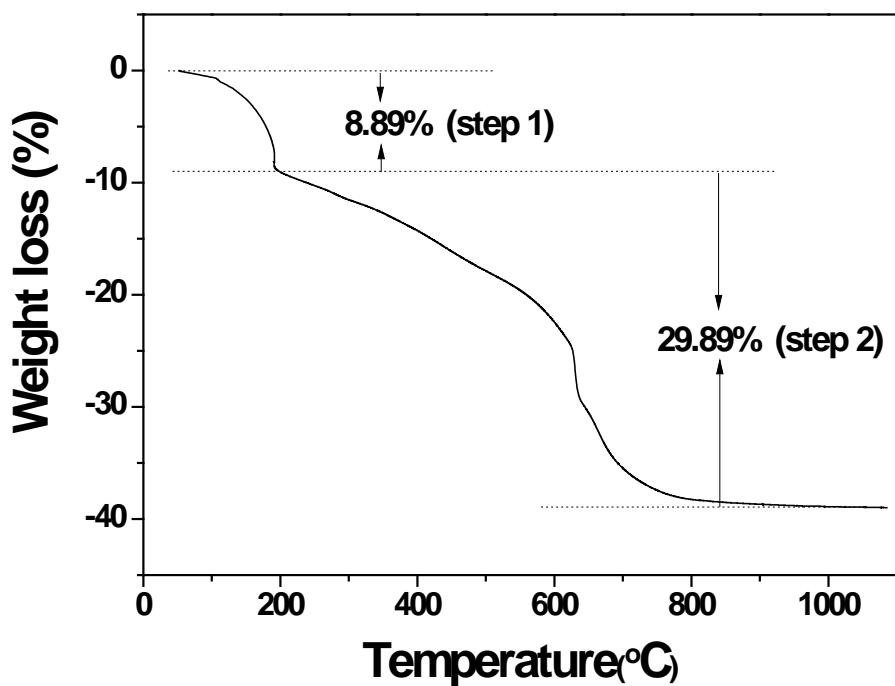


Fig. S2 TG curve for the $(Y_{0.95}Tb_{0.04}Eu_{0.01})(OH)CO_3 \cdot nH_2O$ sample (Figure 1c), where n was found to be 0.92 from step 1 of weight loss.

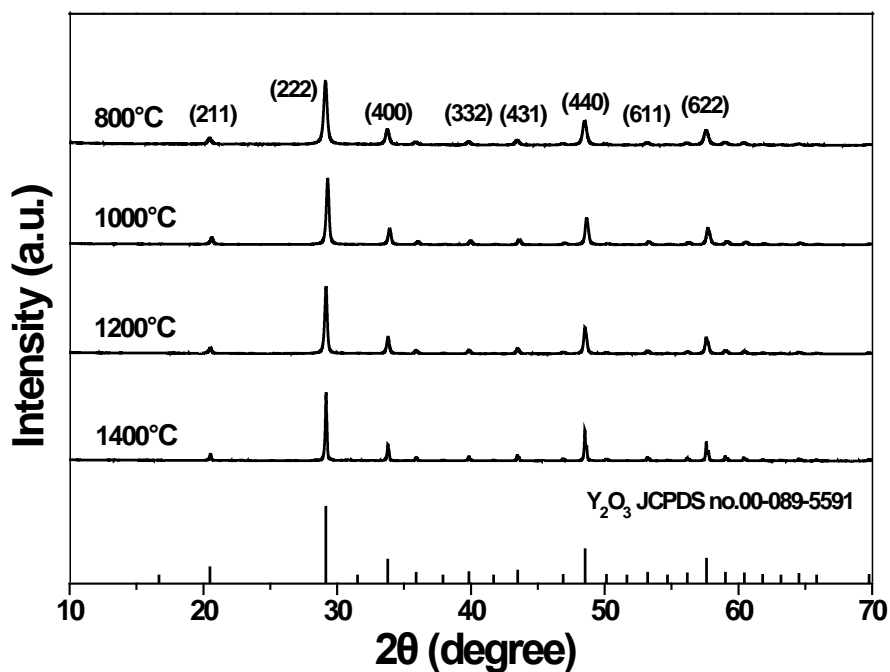


Fig.S3 XRD patterns of the products calcined from $(Y_{0.95}Tb_{0.04}Eu_{0.01})(OH)CO_3 \cdot 0.92H_2O$ (Figure 1c) at various temperatures.

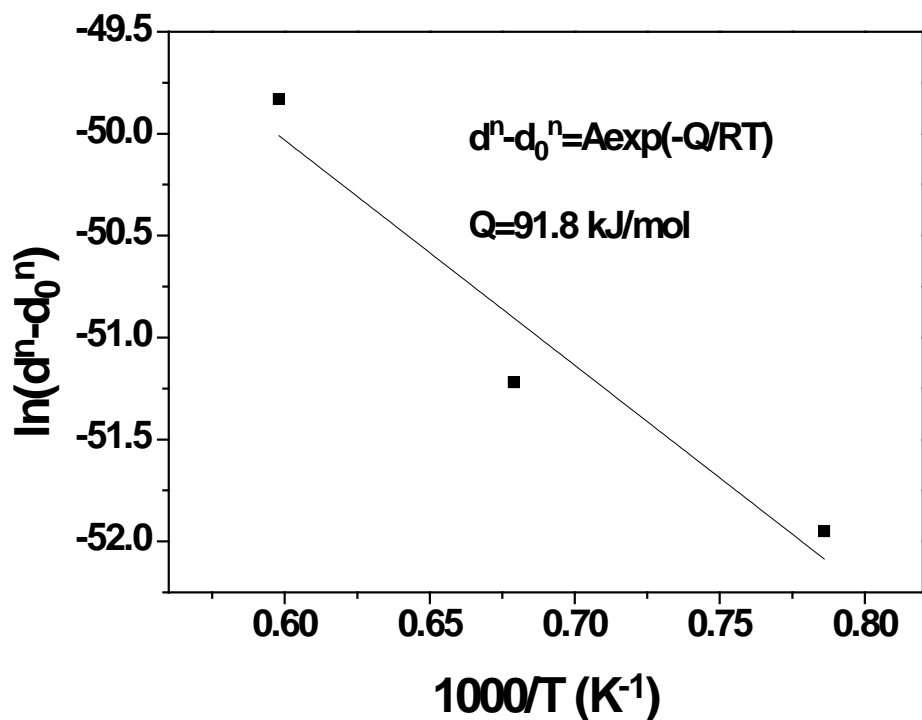


Fig.S4 Plot of $\ln(d^n - d_0^n)$ versus $1/T$ for crystallite growth. In the equation $d^n - d_0^n = A \exp(-Q/RT)$, d and d_0 are the grain size and the size value of the 800 °C product, respectively, A is a constant, R is the gas constant, T is the temperature in Kelvin, and Q is the activation energy for growth. The results are better fitted with $n=3$ in this work.

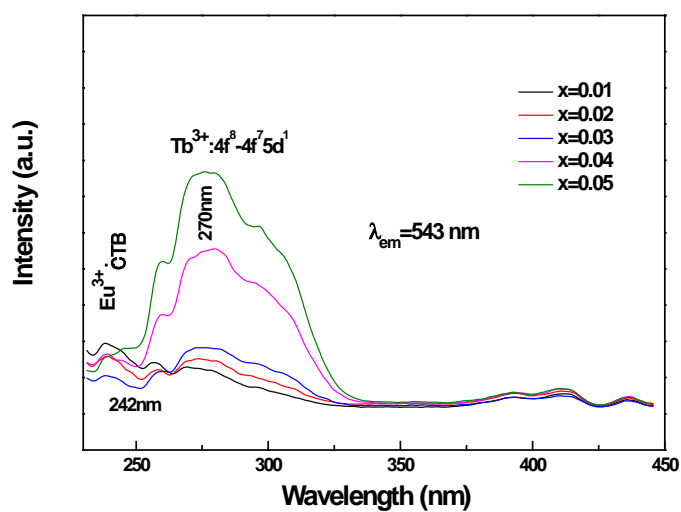


Fig.S5 Photoluminescence excitation spectra of $(Y_{0.95}Tb_xEu_{0.05-x})_2O_3$.

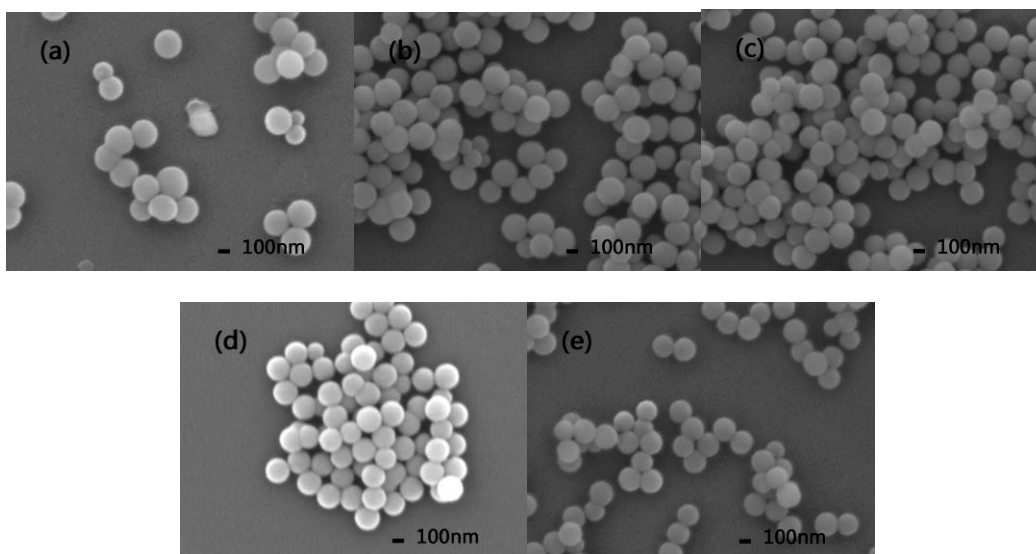


Fig.S6 FE-SEM micrographs showing the morphologies of $(Y_{0.98-y}Tb_{0.02}Eu_y)(OH)CO_3 \cdot nH_2O$, with (a) $y=0.005$, (b) $y=0.01$, (c) $y=0.02$, (d) $y=0.03$, (e) $y=0.04$.

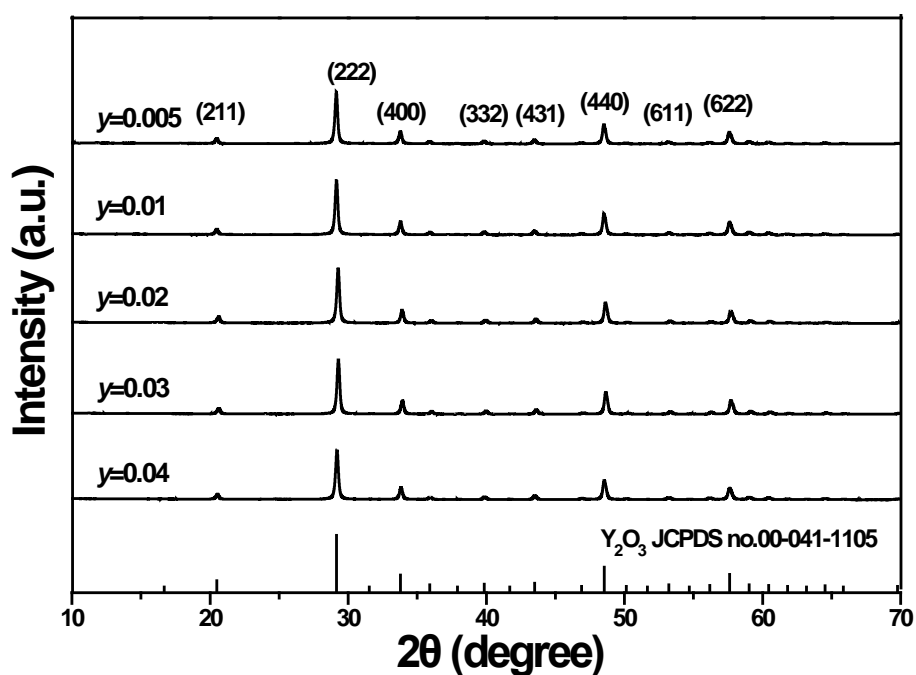


Fig. S7 XRD patterns of the $(Y_{0.98-y}Tb_{0.02}Eu_y)_2O_3$ powders calcined at 1000 °C.

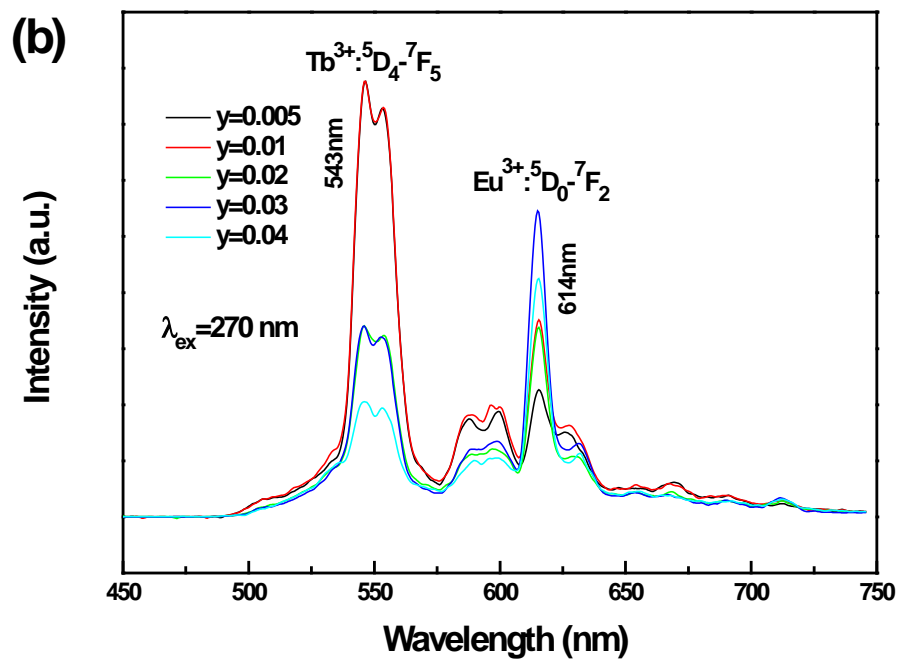
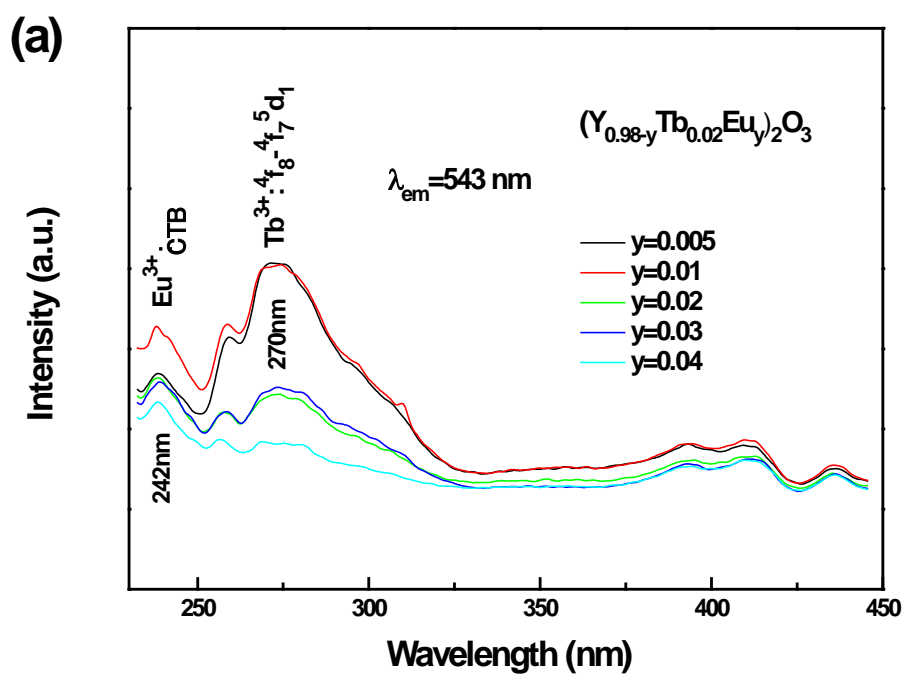


Fig.S8 Photoluminescence excitation (a) and emission (b) spectra of $(Y_{0.98-y}Tb_{0.02}Eu_y)_2O_3$.

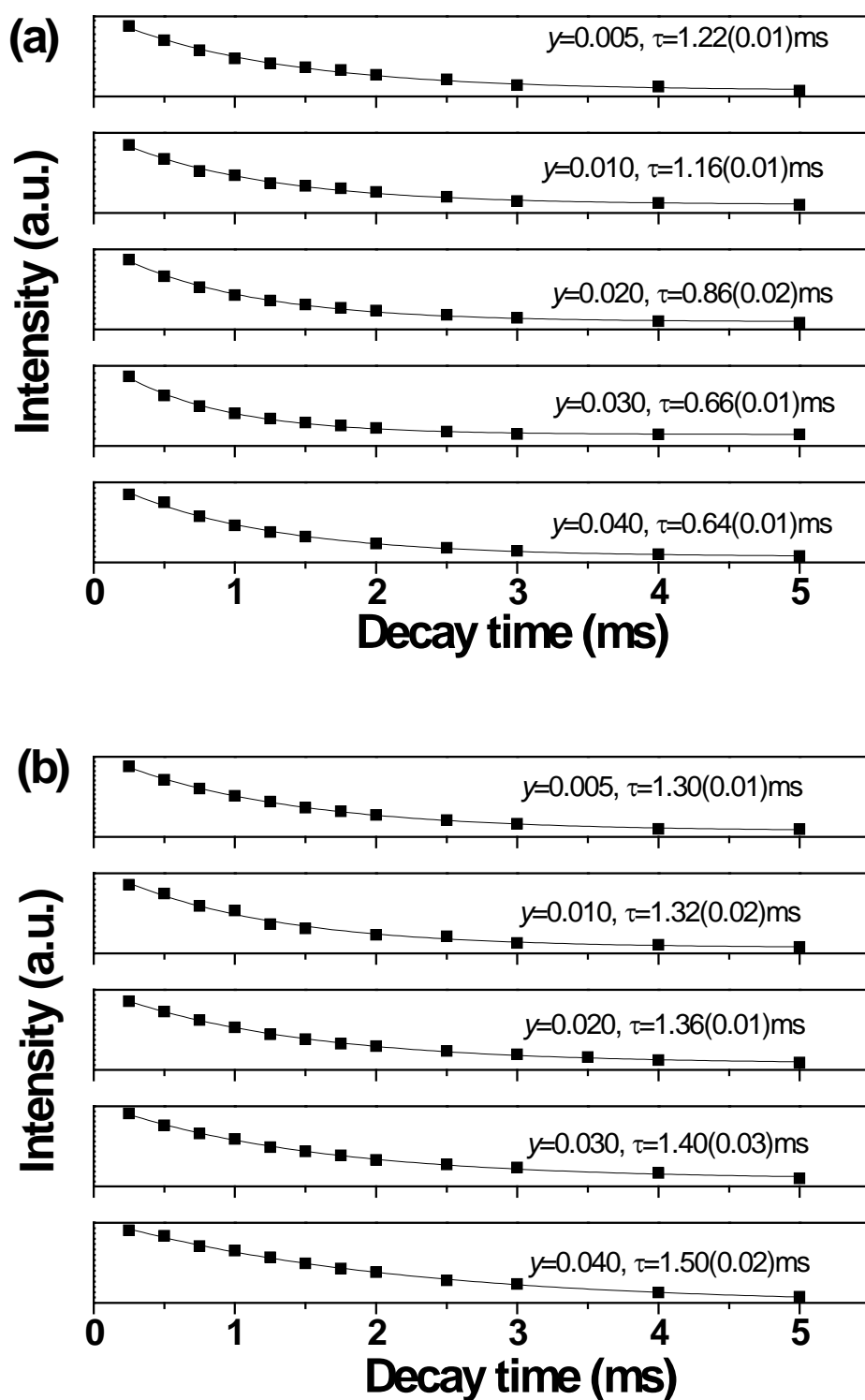


Fig. S9 Fluorescence decay curves of the $(Y_{0.98-y}Tb_{0.02}Eu)_yO_3$ samples and the results of fitting according to the single exponential of $I = A \exp(-t/\tau) + B$, where A and B are constants, I is the emission intensity, t the decay time, and τ the fluorescence lifetime. Parts (a) and (b) are for the 545 nm Tb^{3+} emission and the 614 nm Eu^{3+}

emission, respectively. For the lifetime, the number in bracket represents the value error.

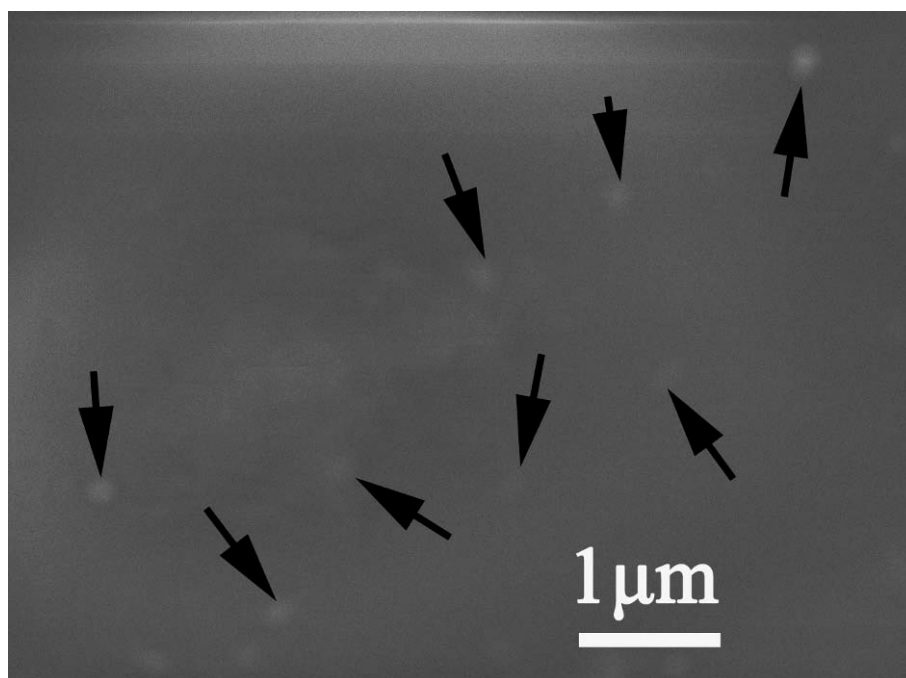


Fig.S10 FE-SEM micrograph showing morphology of the polymer film with $(Y_{0.95}Eu_{0.05})_2O_3$ spheres as fillers. The white objects pointed by arrows are the oxide spheres. As most of the spheres are buried in the interior of PVA, only those at or close to the film surface are unambiguously identifiable.